JCHR (2019) 9(3), 225-234

Journal of Chemical Health Risks

www.jchr.org

ORIGINAL ARTICLE

Enhancing the Antimicrobial Properties Copper Oxide Shell with the Magnetic Mesoporous Core- Shell

Seyed Kamal Rajabi, Shabnam Sohrabnezhad*

Department of Chemistry, Faculty of Science, Guilan University, P.O. Box 1914, Rasht, Iran

(Received: 22 January 2019 Accepted: 3 June 2019)

KEYWORDS

Mesoporous core-shell;
Post-synthesis;
Magnetite;
Antimicrobial agent *i*

ABSTRACT: In this work, Magnetic Fe_3O_4@MCM-41/CuO nanocomposite was preparation of iron oxide magnetite nanoparticles and development of MCM-41 mesoporous shells on the surface of iron oxide magnetite after Fe_3O_4@MCM-41 was organofunctionalized and finally formation CuO shells with thickness ~ 25-30 nm in the surface of Fe_3O_4@MCM-41-NH_2 core-shell. The properties of prepared magnetic core-shell were characterized by transmission electron microscopy (TEM), X-ray diffraction (XRD), nitrogen adsorption–desorption measurement and vibration sample magnetometer (VSM). The applicability of the synthesized core-shell was tested as an antimicrobial agent against gram-positive and gram-negative bacteria. It was showed that the Fe_3O_4@MCM-41@CuO act as an ideal antimicrobial agent in compared with that of the pure copper oxide and Fe_3O_4@CuO.

INTRODUCTION

Various metal and metal oxide materials are widely used such as magnetic storage media, solar energy conversion, electronics, sensors, batteries and catalytic converters, which include copper nanoparticles and copper oxides [1, 2]. Nanoparticles (NP) have emerged as a novel alternative to overcome bacterial multidrug resistance encountered globally due to misuse of antibiotics [3]. Use of nanoparticles as antimicrobial agents could overcome mechanisms of bacterial resistance as the microbicidal nature of nanoparticles result from direct contact with the bacterial cell wall, without the need to penetrate into the cell [3]. The development of antibacterial resistance to NPs is therefore less likely when compared to antibiotics. Nanoparticles therefore have potential to be developed into antimicrobial theranostics in medicine [3, 4]. Several methods for the synthesis of copper oxide with different sizes and morphologies, such as vacuum vapor fermentation, solid-phase growth, micro-emulsion and hydrothermal synthesis have been developed [5-7]. However, the synthetic routes that are reported in many sources require plentiful and complex materials, reducing agents and special additives. [1, 2]. The intrinsic and super-antibacterial properties of copper oxide, compared to other antimicrobial agents, are due to longer and longer shelf life, low toxicity, low prices and good environmental environments [1]. Sometimes copper is a selective option used as an agent for water purification and the deactivation of some microorganisms and bacteria [8]. The main problem of copper oxide nanoparticles in industrial applications is the re-collection of refined water that increases industrial costs and contaminates the treated water [9]. To solve the problem of antibacterial magnetic

*Corresponding author: kamal.rajabi048@gmail.com (K. Rajabi)
DOI: 10.22034/jchr.2019.668187

nanocomposites used [9]. Several advantages of using metal oxides as antimicrobial agents can be seen in improving safety and stability in comparison with other antibacterial agents [10]. Day by day, the use of copper and its complexes increases as the effective materials in water treatment, textiles and etc. [11]. Microorganisms are affected by low amounts of copper and their complexes. Due to the insignificant sensitivity of human tissues to copper and its complexes, microorganisms exhibit sensitivity to efficiency even at low concentrations [11].

Considering that pure MCM-41 silicone materials with high surface area, high pore volume, parallel pore structure without network complexity and biocompatibility have been successfully used for such systems as drug delivery control systems and antibacterial carriers [12-17]. Many previous researches have been documented in the introduction of transition metal elements in the mesoporous silica materials to prepare redox catalysts [18]. Two preparative methods are generally available to introduce catalytically active species into the MCM-41 support, as-synthesized and post synthesized [18-20].

Some of the applications of silicon-magnetic nanoparticles include photocatalytic [12, 21 and 22], catalytic [23], and antibacterial [24] properties.

Research shows that due to its unique magnetic properties, low toxicity, good biocompatibility, the combination of magnetic nanoparticles with silicone mesoporous can be a very good option for drug delivery systems [25, 26]. In recent research, the synthesis of mesoporous silicon nanocomposites with magnetic properties, either in the form of core-shell or as a non-magnetic magnetic material [24-27] also copper deposition on mesoporous silicon oxide and other metal oxides [12] has been reported. To the best of our knowledge, there is no report on the controlled synthesis of Fe_3O_4@MCM-41@CuO core-shell as an antibacterial agent. Herein, in this study, a hybrid of a magnetic Fe_3O_4 cores along with MCM-41 shells and CuO shells was constructed [24]. However, Fe_3O_4@MCM-41@CuO not only shows high efficiency and selectivity towards the antimicrobial activity but also can be separated and recovered efficiently from the reaction solution by applying external magnetic fields .

MATERIALS AND METHODS

Materials

Tetraethylorthosilicate (TEOS, 98%), ammonia (25 wt.%), the surfactant Cetyltrimethylammonium bromide (CTAB), 3- aminopropyltriethoxysilane(APTES), copper (II) nitrate($Cu(NO_3)_2$. $3H_2O$), sodium hydroxide (NaOH), sodium fluoride (NaF), Ferric trichloride hexahydrate, ethylene glycol (EG), ammonium acetate, and ethanol were purchased from Fluka and Merck (Darmstadt, Germany).

Synthesis of magnetic Fe_3O_4@MCM-41@CuO core-shell

The synthesis of Fe_3O_4@CuO core-shell, Fe_3O_4 core and CuO NPs was done according to the previous literatures [1, 28 and 29]. To synthesize Fe_3O_4@MCM-41 [29], 3 g of the synthesized Fe_3O_4 NPs was dispersed in a mixture of ammonia solution (10 mL, ammonia 25% and distilled water 100 mL) in a beaker at 40 °C. Then, 20 mL TEOS, 0.9 g NaOH and 0.2 g sodium fluoride and 14 g CTAB were added to the mixture and stirred for 2 h. Then the mixture was stirred at 40 °C for 2 h. Finally the magnetic composite in an autoclave was treated at 120 °C for 48 h. The resultant solid was filtered, washed with distilled water and dried at 60. After, the synthesized particles calcined for 3 h at 500°C.

Organofunctionalization of Fe_3O_4@MCM-41 was carried out according to literature [18]. In brief, 4.0 g synthesized Fe_3O_4@MCM-41 was charged into a round flask Containing 120 mL toluene and then 6.0 mL of 3-aminopropyltriethoxysilane was added drop wise. The reflux was performed for 8 hours. The resulting solid was separated by magnet, washed with ethanol and distilled water several times, and dried at room temperature for 12h. To prepare Fe_3O_4@MCM-41@CuO core-shell, 120 ml of copper (II) nitrate solutions was mixed with (0.02 M) with 2.0 g NH_2functionalization Fe_3O_4@MCM-41 [12, 18]. The mixture was stirred constantly at room temperature for 24h. The solid product was washed with distilled water several

times and dried at 50°C. Eventually dried solid product calcined in a furnace at 550°C in air for 6h.

Evaluation of antibacterial properties

Fe_3O_4, CuO, Fe_3O_4@CuO, Fe_3O_4@MCM-41 and Fe_3O_4@MCM-41@CuO were diluted in different concentrations (2 to 200 µg/ml) using ethanol and then added to well microplates [24]. 0.5 McFarland of *K. pneumoniae ESBL producer*, *non-ESBL producing K. pneumoniae*, *ESBL producing E. coli*, *E. coli bl21* (free plasmid), *MRSA*, *MSSA*, *MBL producing P. aeruginosa* and *non MBL producing P. aeruginosa* were prepared and added to each well. Then different values (2-200 µg/mL) of antimicrobial candidate in each well added to 0.5 McFarland of each bacterium and subjected to evaluation for Minimum inhibitory concentration (MIC) and Minimum bactericidal concentration (MBC) [30]. Bacteria in presence and absence of antimicrobial candidate were positive and negative control respectively. Microplates incubate conditions were at 37˚C for 24h. The turbidity was evaluated at 570nm by ELISA reader (enzyme-linked immune sorbent assay). To determine the MBC, the MIC value and higher concentration were cultivated on nutrient agar. CFU/ml of each bacterium was obtained in comparison with McFarland standard, [30].

Characterizations

The Magnetic Mesoporous materials for investigation constructed properties were characterized using a variety of techniques. See Electronic Supplementary information (ESI) for more details.

RESULTS AND DISCUSSION

Characterization of core-shell

The x- ray diffraction patterns of the fabricated core-shells, copper oxide (CuO) and magnetite nanoparticles were presented in Figure 1. The XRD pattern of synthesized Fe_3O_4 cores showed (Figure 1a) that Diffraction peaks 35.058˚ (311), 43.293˚ (400), 55.312˚ (422), 57.589˚ (411), 63.190˚ (440) and 74.081˚ (533) correspond to different planes of cubic phase of Fe_3O_4 [31]. According by Scherer's formula [29, 32], the average crystal size of Fe_3O_4 core was 12 nm. The XRD pattern for copper oxide can be showed (Figure 1b) by the characteristic 32.67˚, 35.63˚, 38.90˚, 48.83˚, 53.60˚, 58.24˚, 61.59˚, 66.5˚ and 68.19˚ refer to (111), (002), (-111), (-202), (020), (202), (-113), (022), (220) respectively that illustrates of monoclinic phase of copper oxide [24, 29]. The XRD pattern of synthesized Fe_3O_4@MCM-41 core-shell indicated (Figure 1c) Diffraction peaks 30.23˚, 35.73˚, 43.31˚, 57.21˚ and 62.47˚ corresponds to(220), (311), (400), (411) and (440) planes of cubic phase of Fe_3O_4 and one strong diffraction peak at 2.75˚ refer to (100) plane of hexagonal structure from MCM-41 [12]. The XRD pattern of Fe_3O_4@MCM-41@CuO core-shell (Figure 1d) showed peaks that could be indexed to MCM-41 structure, copper oxide and Fe_3O_4. The broadening of core-shell peaks in comparison with magnetite core and copper oxide alone could be related to the quantum size effect of core-shell. Using Scherer's formula [12, 29], calculated average crystal size of MCM-41 and CuO shells and obtained 27.72 and 14.00 nm, respectively.

In Figure 2, Spectrums FTIR very well were introduced structure of Fe_3O_4@MCM-41/CuO core-shell and other perpetrated nanocomposite. The bands at 3430 cm^{-1} and 557 cm^{-1} in Figure 2a and Figure 2b, are corresponding to O–H stretching and Fe–O bond respectively. Also band 1625 cm^{-1} was attributed to the bending vibration of water in the Fe_3O_4 nanoparticles [33, 12, and 34]. In Figuer 2b, Figure 2c, Figure 2d, peaks 1072.33, 800.76 and 450.95 cm^{-1} can be owned to Si–O–Si bending and stretching vibrations [12, 18]. The weak peaks at 2338.92 cm^{-1}, 2854.46 cm^{-1}, and 2925.63 cm^{-1} were assigned to the vibrations of atmospheric CO_2 and the symmetry and asymmetry stretching vibrations of $–CH_2–$, respectively [12, 34]. In addition, in Figure 2c the peaks 2935, 2837.5 cm^{-1} and 1567 cm^{-1} can be attributed to asymmetric and symmetric vibrations of $–CH_2$ group of APTES molecules and amine groups, respectively. Accordingly, they show surface of Fe_3O_4@MCM-41 by APTES was successfully functionalized [18, 35]. Usually, three peaks in the range of

400–700 cm^{-1} indicate CuO nanostructures [36]. In Figure 2d, peaks 469.04 and 586.47 cm^{-1} can be corresponded to the Fe-O and Cu-O stretching vibration of Fe_3O_4 and CuO, respectively. All bands in Fe_3O_4@MCM-41/CuO sample shift to higher wave numbers and increased intensity (except peak at 3328.55 cm^{-1}). This can be related on core-shell structure [12]. The particle sizes and the morphologies of the samples were illustrated by using SEM and TEM. SEM images for Fe_3O_4@MCM-41 core-shell indicated a smooth surface and slightly rough one for Fe_3O_4@MCM-41@CuO core-shell due to copper oxide shells (Figure 3). The EDX spectra (Figure 3) of the samples explained loading of copper oxide in Fe_3O_4@MCM-41 core-shell Based on peaks Cu, Fe, Si and O. results EDX showed which weight percentage (wt. %) of magnetite cores, Mesoporous and copper oxide shells were calculated 70.48, 21.05 and 10.16%, respectively.

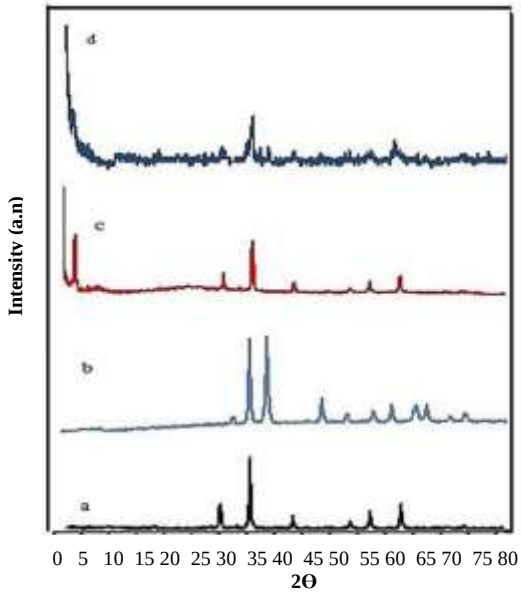

Figure 1. XRD patterns for Fe_3O_4 (a), CuO (b), Fe_3O_4@MCM41(c) and Fe_3O_4@MCM41@CuO nanoparticles (d).

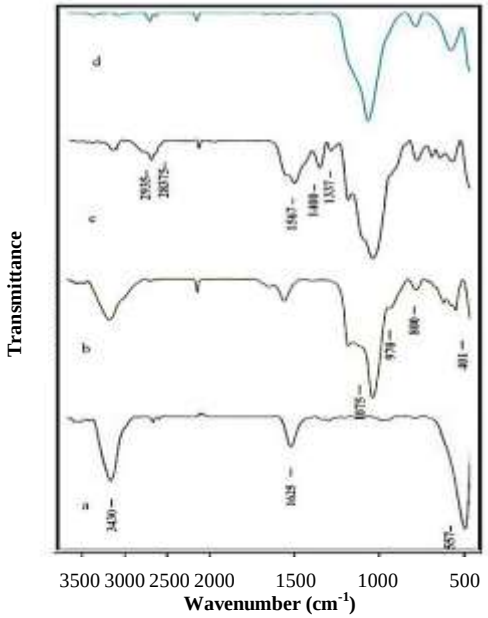

Figure 2. FTIR spectra of the Fe_3O_4 (a), Fe_3O_4@MCM41 (b), Fe3O4@MCM41-NH_2 (c), Fe3O4@MCM41/CuO (d) nanocomposite.

The TEM images for core-shells were showed, presented the Fe_3O_4 cores (the black part) with diameter size between 15-20 nm and surrounded shells of MCM-41 material(~ 5-10 nm) and copper oxide average with thickness ~25-30 nm (Figure 4). The porous properties of magnetic core-shells samples were examined by measuring the nitrogen adsorption isotherms (Figure S5). The Fe_3O_4@MCM-41 core-shell isotherm is of type IV according to the IUPAC classification of adsorption isotherms [12, 36], typical of mesoporous solids. The Brunauer–Emmett–Teller surface area (S_{BET}) Fe_3O_4@MCM-41core-shell was $895 m^2 g^{-1}$. Also the pore diameter and pore volume were 2.7 nm and 0.71 mL g^{-1}, respectively. These results indicated the presence of MCM-41 mesoporous in the new core-shell [12, 36]. The BET surface area of the copper oxide, magnetic cores according with literature [36] were13.8 and 0.32 m^2 g^{-1} respectively and Fe_3O_4@MCM-41@CuO core-shell [12] was calculated 750 m^2 g^{-1}. These results were in agreement with other articles [12, 33- 34]. To appraise the magnetic behavior of the magnetic core-shells, the magnetic measurements were carried out at 300 K. The saturation magnetization values (Ms.) of the Fe_3O_4 MNPs, Fe_3O_4@MCM-41 and Fe_3O_4@MCM-41@CuO core-shells were measured to be 73.65, 23.20 and 1.84 $emug^{-1}$, respectively (Figure 6). The decrease ofthe saturation magnetization is most probably related to the he growth of the CuO shells and MCM-41 shells on the surface on the surface of Fe_3O_4 nanoparticles [37]. Moreover, coercive force (Hc.) of 50.0, 52.0 and 90.0 Oe and remnant magnetization (Mr.) of 4.89, 2.40 and 0.70 emu g^{-1} were obtained for Fe_3O_4, Fe_3O_4@MCM-41 and Fe_3O_4@MCM-41@CuO core-shells, respectively. These results reflect ferromagnetic character [38]. The Fe_3O_4@MCM-41@CuO core-shell can be easily dispersed in aqueous solution and remains in suspension until exposed to a magnetic field, because it's the low coercively and remanence.

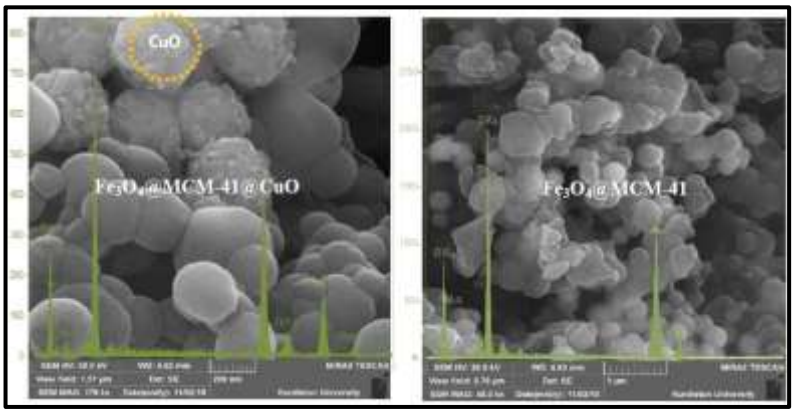

Figure 3. SEM images and EDX spectra of core-shells.

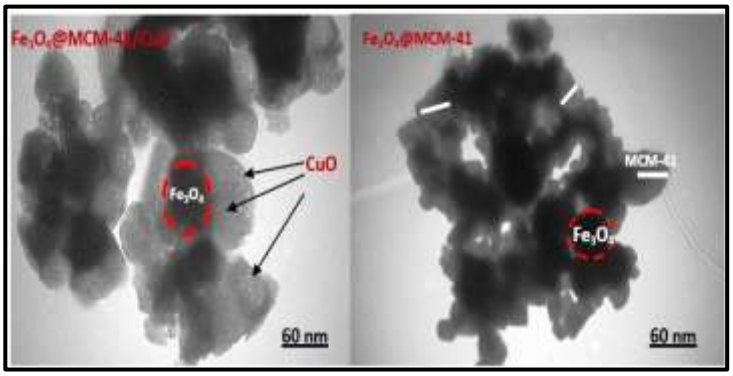

Figure 4. TEM images of core-shells

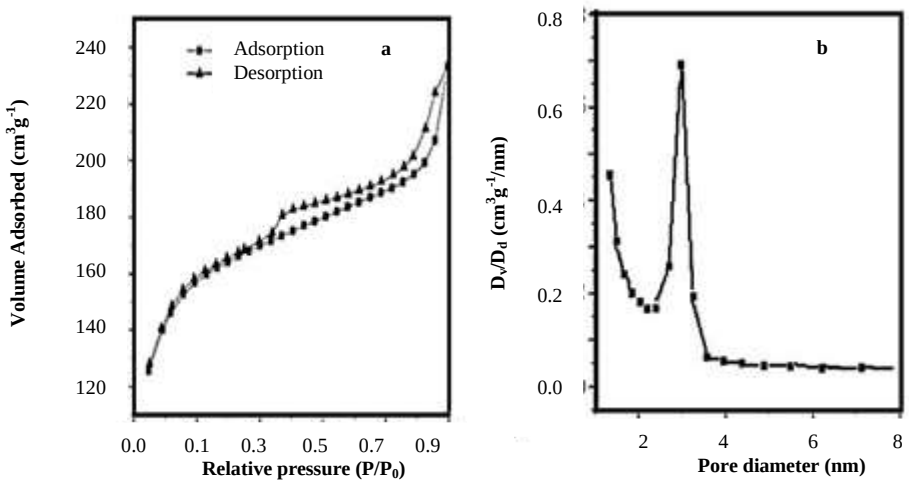

Figure 5. (a) Nitrogen adsorption-desorption isotherms and (b) Pore size distribution of the Fe_3O_4@MCM-41 [25].

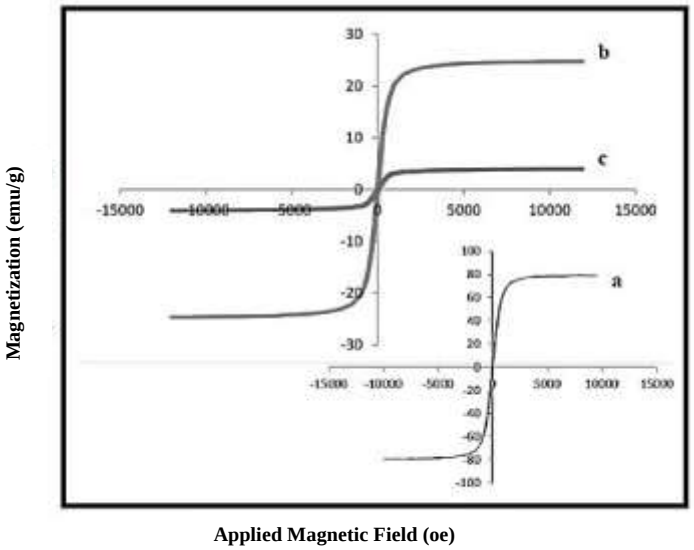

Figure 6. Hysteresis loops recorded of (a) Fe_3O_4, (b) Fe_3O_4@MCM-41 and Fe_3O_4@MCM41/CuO from solution under an external magnetic field.

Antibacterial mechanism

The results showed that antimicrobial activities of samples and core-shells against studied bacteria were Fe_3O_4@MCM-41@CuO, Fe_3O_4@CuO and CuO NPs respectively. Based on the results, magnetite cores and Fe_3O_4@MCM-41 core-shell did not display antimicrobial activity (Table 1).Several possible antimicrobial mechanisms of metal and metal oxide NPs have been summarized in the latest studies [39]. It has been reported that, copper (II) ions released from copper oxide surface in aqueous phase are responsible for antimicrobial activity of the materials [40]. According physiologic conditions, bacterial cell walls are negatively charged by functional groups such as carboxyl's, phosphate and hydroxyl in lipoproteins at the surface [24, 41]. By binding the Cu^{2+} ions with the functional groups of proteins and enzymes the cell process gets inactive and inhibited. This is the main reason for the antimicrobial property of the synthesized copper oxide and Fe_3O_4@MCM-41@CuO core-shell.

The magnetic Fe_3O_4@MCM-41 core-shell together with copper oxide shell showed extraordinary antimicrobial properties against studied bacteria. This increase in antimicrobial activity can be attributed to two factors:

1. MCM-41 as a Porous surface not only prevents copper oxide aggregation which in turn barricades the release of large amount of copper (II) ions and the decrease in antimicrobial activity CuO NPs but also causes uniformity of distribution[24, 42].

2. Copper oxide particles in the magnetic mesoporous with their smaller sizes (average crystal size ~14 nm) in comparison to other copper oxide nanoparticles reported in Table 1 can release large amounts of copper (II) ions in shells [24, 42]. Findings

Table 1. Investigation antibacterial activity of samples.

Samples	Fe_3O_4	CuO	Fe_3O_4@CuO	Fe_3O_4@MCM-41	Fe_3O_4@MCM-41@CuO
Bacteria	MIC (MBC) µg.mL^{-1}	MIC (MBC) µg.mL^{-1}	MIC (MBC) µg.mL^{-1}	MIC (MBC) µg.mL^{-1}	MIC (MBC) µg.mL^{-1}
E.coli bl21	**-(-)**	100(100)	30(30)	**-(-)**	5(5)
E.coli producing ESBL	**-(-)**	150(155)	55(60)	**-(-)**	6(10)
K. pneumoniae ESBL producer	-(-)	90(100)	60(65)	-(-)	8(8)
non-ESBL producing K. pneumonia	-(-)	75(80)	50(55)	-(-)	8(8)
MSSA	-(-)	85(90)	40(40)	-(-)	5(5)
MRSA	-(-)	140(150)	65(70)	-(-)	6(6)
MBL producing P. aeruginosa	-(-)	180(200)	80(80)	-(-)	10(10)
non MBL producing P. aeuginosa	-(-)	185(200)	75(80)	-(-)	7(7)

Demonstrate that Fe_3O_4@MCM-41/CuO core-shell indicated strong antimicrobial activity at an early stage in comparison to other antimicrobial materials including Fe_3O_4@CuO core-shell (Table 2). According to the recent researches [1, 24] crystal size of copper oxide in new core-shells is smaller than Fe_3O_4@CuO core-shell (~22 nm) [1].

Figure7 shows the results of tests MBC. In Figure 7A, two plates are seen; one contains Staphylococcus aureus and Fe_3O_4@MCM-41 core-shell and the other one contains Fe_3O_4 @ MCM-41 / CuO and Staphylococcus aureus. The sign of bacterial growth; turbidity in the first plate was seen while no bacterial growths was observed in the second plate. In Figure 7B, the plate containing E. coli bacteria and Fe_3O_4 @ MCM-41 got turbid whereas the other plate containing Fe_3O_4 @ MCM-41 @ CuO samples and *E. coli* bacteria showed no bacterial growth which is the sign of Fe_3O_4 @ MCM-41 @ CuO positive response to antibacterial activity.

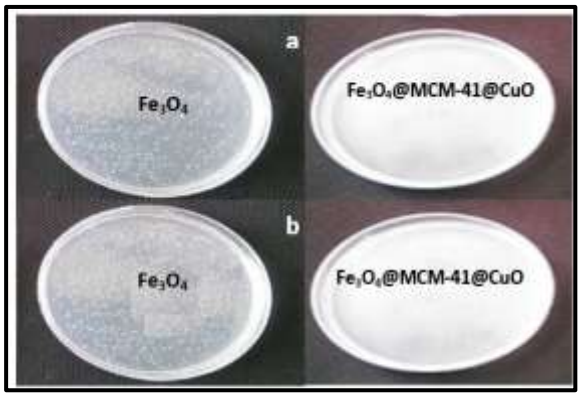

Figure 7. MBC result: Staphylococcus aureus bacteria (a), E. coli bacteria (b).

Table 2. The comparison of antimicrobial activities different

Antimicrobial agent	MIC	Reference
CuO microspheres	500 mg/L	[43]
CuO/TiO_2 nano fibers	45000 mg/L	[10]
Fe_3O_4@CuO	40 mg/L	[1]
Fe_3O_4@MOR@CuO	17.5 mg/L	[24]
Fe_3O_4@MCM-41@CuO	5 mg/L	*Current work*

CONCLUSIONS

In this work, we have suggested a new protocol for the efficient synthesis of Fe_3O_4@MCM-41@CuO core- shell for antimicrobial activity. To the best of our knowledge, this is the first report on antimicrobial activity Fe_3O_4@MCM-41@CuO core- shell against Gram positive (G+) and Gram negative (G-) bacteria. Highlight results in this study include, phenomenal antimicrobial properties of Fe_3O_4@MCM-41@CuO core- shell and easy separation of them using an external magnetic field due to the magnetism of the Fe_3O_4. Nanocomposite characterized by TEM, SEM, XRD, FTIR, BET, VSM and EDX. TEM images confirm XRD spectrums and illustrate the magnetite cores covered with MCM-41 and copper oxide shells.

ACKNOWLEDGEMENTS

The authors are thankful to the post-graduate office of Guilan University for the support of this work.

REFERENCES

1. Rajabi S.K., Sohrabnezhad Sh., Gaphourian S., 2016. Fabrication of Fe_3O_4@CuO core-shell from MOF based materials and its antibacterial activity. Solid State Chem. 244, 160-163.

2. Wang W.W., Zhu Y.J., Cheng G. F., Huang Y.H., 2006. Microwave-assisted synthesis of cupric oxide Nanosheet and Nano whiskers. Materials Letters. 60, 609- 612.

3. Wang, L., C. Hu, and L. Shao, 2017. The antimicrobial activity of nanoparticles: present situation and prospects for the future. Int J Nanomed, 12, 1227-1249.

4. Fernando SSN, Gunasekara TDCP, Holton J., 2018. Antimicrobial Nanoparticles: applications and mechanisms of action. Sri Lankan Journal of Infectious Diseases, 8, 2-11.

5. Mao L.Q., Yamamoto K., Zhou W.L., Jin L.T., 2000. Electrochemical Nitric Oxide Sensors Based on Electropolymerized Film of M(salen) with Central Ions of Fe, Co, Cu, and Mn. Electroanalysis, 12, 72–77.

6. Zhang Y.F., Qiu L.G., Yuan Y. P., Zhu Y.J., Jiang X., Xiao J.D., 2014. Magnetic Fe_3O_4@C/Cu and Fe_3O_4@CuO core–shell composites constructed from MOF-based materials and their photocatalytic properties under visible light. Applied Catalysis B: Environmental. 144, 863–869.

7. Chen Z.F., Meyer T.J., 2013. Copper (II) catalysis of water oxidation. Angew Chem., 125, 728–731.

8. Akhavan O., Ghaderi E., 2010. Cu and CuO nanoparticles immobilized by silica thin films as antibacterial materials and photocatalysts. Surface and Coatings Technology. 205, 219-223.

9. Ding J., Liu L., Xue J., Zhou Z., He G., Chen H., 2016. Low-temperature preparation of magnetically separable Fe_3O_4@CuO-RGO core-shell heterojunctions for high-performance removal of organic dye under visible light. J Alloys and Compounds. 688, 649-659.

10. Youssef A., Barakat N.A.M., Amna T., Al-Deyab S.S., Hassan M.S., Abdel-hay A., Kim H.Y., 2012. Inactivation of pathogenic Klebsiella pneumoniae by CuO/TiO_2 nanofibers: A multifunctional nanomaterial via one-step electro spinning. Ceramics International. 38, 4525-4532.

11. Das D., Chandra Nath B., Phukon P., KumarDolui S., 2013. Synthesis and evaluation of antioxidant and antibacterial behavior of CuO nanoparticles. Colloids Surf B Bio interfaces. 101, 430-433.

12. Sohrabnezhad Sh., Rajabi S.K., 2018. The influence of MCM-41 mesoporous shell in photocatalytic activity of magnetic core-shell. J Photochem Photobiol A. 350, 86–93.

13. Li Z., Barnes J.C., Bosoy A., Stoddart J.F., Zink J.I., 2012. Mesoporous silica nanoparticles in biomedical applications. Chem Soc Rev. 41, 2590−2605.

14. Vivero Escoto J.L., Slowing I.I., Wu C.W., Lin V.S.Y., 2009. Photo induced intracellular controlled release drug delivery in human cells by gold-capped mesoporous silica nanosphere. J Am Chem Soc. 131, 3462−3463.

15. Trewyn B.G., Slowing I.I., Giri S., Chen H.T., Lin V.S.Y., 2007. Synthesis and functionalization of a mesoporous silica nanoparticle based on the sol-gel process and applications in controlled release. Acc Chem Res. 40, 846−853.

16. Trewyn B.G., Whitman C.M., Lin V.S.Y., 2004. Morphological Control of Room-Temperature Ionic Liquid Templated Mesoporous Silica Nanoparticles for Controlled Release of Antibacterial Agents. Nano Letter. 4, 2139−2143.

17. Sobczak I., Ziolek M., Renn M., Decyk P., Nowak I., Katuri M., Lavalley J.C., 2004. Cu state and behaviour in MCM-41 mesoporous molecular sieves modified with copper during the synthesis—comparison with copper exchanged materials. Micropor Mesopor Matter. 74, 23-36.

18. Hao X.Y., Zhang Y.Q., Wang J.W., Zhou W., Zhang C., Liu Sh., 2006. A novel approach to prepare MCM-41 supported CuO catalyst with high metal loading and dispersion. Micropor Mesopor Matter. 88, 38–47.

19. Lu W.J., Lu G.Z., Luo Y., 2002. A novel preparation method of ZnO/MCM-41 for hydrogenation of methyl benzoate. J Mol Catal A: Chem. 188, 225-231.

20. Arruebo M., Galan M., Navascues N., Tellez C., Marquina C., Ibarra M.R., 2006. Development of Magnetic Nanostructured Silica-Based Materials as Potential Vectors for Drug-Delivery Applications. Chem Mater. 18, 1911-1919.

21. Mihai G. D., Meynen V., Mertens M., Bilba N., Cool P., Vansant E. F., 2010. ZnO nanoparticles supported on mesoporous MCM-41 and SBA-15: a comparative physicochemical and photocatalytic study. J Mater Sci, 45, 5786–5794.

22. Nanda B., Amaresh C.P., Parida K.M., 2017. Fabrication of mesoporous CuO/ZrO_2-MCM-41 nanocomposites for photocatalytic reduction of Cr(VI). Chemical Engineering Journal. 316, 1122-1135.

23. Pourhasan-Kisom R., Shirini F., Golshekan M., 2018. Introduction of organic/inorganic Fe_3O_4@MCM-41@Zr-piperazine magnetite nanocatalyst for the promotion of the synthesis of tetrahydro-4H-chromene and pyrano[2,3-d] pyrimidinone derivatives. Applied Organometallic Chemistry. 32, e4485.

24. Rajabi S.K., Sohrabnezhad Sh., 2018. Fabrication and characteristic of Fe_3O_4@MOR@CuO core-shell for investigation antibacterial properties. J Fluorine Chem. 206, 36–42.

25. Dong A., Huang J., Lan S., Wang T., Xiao L., Wang W., Zha T., Zheng X., Liu F., Gao G., Chen Y., 2011. Synthesis of N-halamine-functionalized silica–polymer core–shell nanoparticles and their enhanced antibacterial activity. Nanotechnology. 22, 295602-295611.

26. Padervand M., Gholami M.R., 2013. Removal of toxic heavy metal ions from waste water by functionalized magnetic core–zeolites shell nanocomposite as adsorbents. Environmental Science and Pollution Research. 20, 3900-3909.

27. Padervand M., Janatrostami S., Kiani Karanji A., Gholami M.R., 2014. Incredible antibacterial activity of noble metal functionalized magnetic core–zeolitic shell nanostructures. Mater Sci Eng C. 35, 115-121.

28. Sohrabnezhad Sh., Valipour A., 2013. Synthesis of Cu/CuO nanoparticles in mesoporous material by solid state reaction. Spectrochimica Acta Part A, 114, 298–302.

29. Khorshidi A., Shariati Sh., 2014. Sulfuric acid functionalized MCM-41 coated on magnetite nanoparticles as a recyclable core–shell solid acid catalyst for three-component condensation of indoles, aldehydes and thiols. RSC Adv. 4, 41469-41469.

30. Balouiri M., Sadiki M., Ibnsouda S.K., 2016. Methods for in vitro evaluating antimicrobial activity: A review Pharm Anal. 6, 71-79.

31. Jafarzadeh A., Sohrabnezhad Sh., Zanjanchi M.A., Arvand M., 2016. Synthesis and characterization of thiol-functionalized MCM-41 nanofibers and its application as photocatalyst. Micropor Mesopor Mater. 236, 109-119.

32. Zhang T., Lin L., Zhang X. , Liu H., Yan X., Qiu J., Yeung K.L., 2015. Synthesis and characterization of ZIF-8@SiO_2@Fe_3O_4 core@double-shell microspheres with noble metal nanoparticles sandwiched between two shell layers. Mater Letter. 148, 17–21.

33. Schwertmann U., Cornell R.M., 2000. Iron Oxides in the Laboratory: Preparation and Characterization, 2nd, Completely Revised and Enlarged Edition. Wiley, New York.

34. Xie W., Ma N., 2009. Immobilized Lipase on Fe_3O_4 Nanoparticles as Biocatalyst for Biodiesel Production. Energy Fuels. 23, 1347–1353.

35. Zhang J.M., Zhai S.R., Zhai B., An Q.D., Tian G., 2012. Crucial factors affecting the physicochemical properties of sol–gel produced Fe_3O_4@SiO_2–NH_2 core–shell nanomaterials. J Sol-Gel Sci Technol. 64, 347–357.

36. Chen X., Lam K.F., Yeung K.L., 2011. Selective removal of chromium from different aqueous systems using magnetic MCM-41 nano sorbents. Chemical Engineering Journal, 172, 728– 734.

37. Kliche G., Popovic Z.V., 1990. Far-infrared spectroscopic investigations on CuO. Phys Rev B. 42, 10060–10066.

38. Moritz M., Geszke-Moritz M., 2013. The newest achievements in synthesis, immobilization and practical applications of antibacterial nanoparticles. Chemical Engineering Journal. 228, 596–613.

39. Azam A., Ahmed A.S., Oves M., Khan M.S., Habib S.S., Memic A., 2012. Antimicrobial activity of metal oxide nanoparticles against Gram-positive and Gram-negative bacteria: a comparative study. Int J Nanomed. 7, 6003-6009.

40. Pandiyarajan T., Udayabhaskar R., 2013. Synthesis and concentration dependent antibacterial activities of CuO nanoflakes. Mater Sci Eng. C, 33, 2020-2024.

41. Ma Z., Ji H., Tan D., Teng Y., Dong G., Zhou J., Qiu J., Zhang M., 2011. Silver nanoparticles decorated, flexible SiO_2 nanofibers with long-term antibacterial effect as reusable wound cover. Colloids Surf. A, 387, 57-64.

42. Wahab R., Tabrez Khan Sh, Dwivedi S., Ahamed M., Musarrat J., AlKhedhairy A.A., 2013. Effective inhibition of bacterial respiration and growth by CuO microspheres composed of thin nanosheets. Colloids Surf. B, 111, 211–217.

43. Liu B.S., Xu D.F., Chu J.X., Liu W., Au C.T., 2007. Deep Desulfurization by the Adsorption Process of Fluidized Catalytic Cracking (FCC) Diesel over Mesoporous Al−MCM-41 Materials. Materials Energy Fuels. 21, 250-255.